OPEN ACCESS

GRS Journal of Multidisciplinary Research and Studies
Abbreviate Tittle- GRS J Mul Res Stud
ISSN *(Online) - 3049-0561*
https://grspublisher.com/journal-details/GRSJMRS

Vol-3, Iss-1 (Jan- 2026)

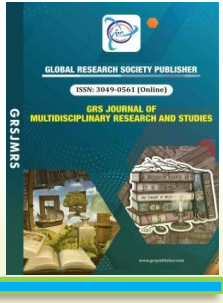

Laminar Convection flow in Warm Bathing Water: An In-depth Review with Flow Parameter Dependent Mixing

Alabodite Meipre George & Biralatei Fawei

[1]Department of Mathematics, Niger Delta University, Wilberforce Island, Bayelsa State, Nigeria.

[2]Department of Computer Science, Niger Delta University, Wilberforce Island, Bayelsa State, Nigeria.

Article History
Received: 17.12.2025
Accepted: 07.01.2026
Published: 18.01.2026

Corresponding Author: Saravanan Venkadasalam

Abstract: Laminar free convection flow in warm bathing water had just been investigated numerically for a range of Reynolds number $0 \leq Re \leq 110$ keeping $Fr = 2.5$ and $Pr = 9.5$ fixed throughout the study. The result showed that cabbeling changes slightly with *Re* owing to the increasing *Re*, even though, the velocity in such free convection flows are usually small. The result showed that volume of hot water at the upper section at some point in time depleted completely and in turn induces the entire ambient water temperature which later became the same temperature everywhere without any external influence. These results require just a little mixing for temperature between $0^{\circ}C$ and $10^{\circ}C$ to attain *Tm*. The time taken for dense fluid to sink to the bed for smaller *Re* is slightly longer as compared to the time it takes as *Re* increases. Temperature profiles were also analysed at some points (X, 69; 30; 10) below the contact layer and plotted against the x-coordinate. In a similar manner, profiles of x-component and y-component velocities were also determined at (X, 69) for the various *Re* cases as considered and plotted against the x-coordinate. Fluctuations in the temperature profiles describes the convection precess as both hot and cold fluid mixes in all direction and continue to deplete further. Meanwhile, fluctuations in the curves for the y-component velocity profile indicates that even as the dense fluid continue to descend, fluid that is still positively buoyant moves upwards. The maximum time taken for descending dense fluid to reach domain floor and the time taken to attain that depth were also considered. From the empirically determined data set, we could identify a single regime of Re-dependence and shown by the straight line in Figs. 7, which represent best fit power law obtained by linear regression of *logRe* on *logτn* (see equation).

Keywords: *Convection flow, Ambient fluid, Temperature of maximum density Tm, Laminar flow, Cabbeling.*

Cite this Article

Saravanan. V, (2025) Design and Fabrication of a Prototype Mobile Offshore Charging Ship (MOCS). *GRS Journal of Multidisciplinary Research and Studies, Vol-3(Iss-1). 01-10*

Introduction

Free convection in fluid are a remarkable kind of fluid movements that are mostly influenced by buoyancy through heat transfer in fluids. Such fluid movement occurs regularly in our environments without any external interference, but due to density difference caused by temperature gradient (Ongodiebi & George, 2025; Ezan & Kalfa, 2017; Khanorkar & Thombre, 2013). Research on free convection flows have received great attention recently based on its significance in our everyday activities and their applications ranging from the technological, scientific and engineering point of view. Example of such include: thermal storage systems, electronic equipment, solar ponds, cooking, over-head water tanks, warm bathing water, ventilation of buildings, Cooling of power plants, etc., (Ongodiebi & George, 2025; Khurshid & Silaipillayarputhur, 2018; Radhwan & Zaki 2000; Djoubeir et al. 2014; Charqui, et al. 2021; Gopalakrishnan et al. 2005). Literature by previous authors with different configurations also suggest that a comprehensive review had been made on convection flows, where theoretical, numerical and experimental results are obtained, describing the evolution of convective flow pattern and temperature profiles with time, and as well the time taken to reach a steady state condition (Charqui, et al. 2021; Cianfrini et al. 2015; Hossain & Rees, 2005). In a system where either the bottom or top horizontal boundaries are heated with temperature $10^{\circ}C$, assuming that the ambient fluid (water) is below the temperature of

Maximum density Tm. Over time, the ambient water at or very close to the heated boundaries will gain heat and this in turn become less dense than it was, forming buoyancy flow. This fluid motion can sometimes be referred to as penetrative convection, inducing the entire ambient water further. Whereas, any fluid at the top boundary that have mixed up to $4^{\circ}C$ or a temperature close to it will sink forming a downward descending plume to the ambient floor. Though, this is also dependent on the height of the domain of computation (Ongodiebi & George, 2025; Kane, 2017; Nayak et al. 2018; Cianfrini et al. 2015).

It is known universally that temperature dependence on water density is non-monotonic. Note that in normal situation, $3.98^{\circ}C$ is the temperature of maximum density Tm for fresh water at atmospheric pressure, sometimes taken to be $4^{\circ}C$ in most numerical calculations; and density differences are small for temperature

variation between 0°C and 10°C. In order to depict a practical flow scenario, the proposal of a laminar flow seemed more appropriate for free convection flow cases. Where the heat transfer rate in such flows are usually dependent on both the geometry and temperature variation in the ambient fluid. This further implies that the choice of flow parameters used during simulations are very crucial knowing that the fluid velocity is usually small. However, transient flow scenario have also been considered in an enclosure, where authors have focused more on determining the existence of multiple stable steady-state or periodically-oscillating flow pattern solutions and little on the heat transfer performance of the domain (Hossain & Rees, 2005; Cianfrini et al. 2015). From the research so far on the study of convection flows, the water is mostly confined with varied fluid volume and as well in different shaped containers; where heat is mostly applied to the water from the top, bottom or the side-walls of the container (Brownridge & Robinson, 2019; Ongodiebi & George, 2025). These authors (Shirvan, 2017; Li et al. 2011; Rahman et al. 2010; Singh et al. 2016; Kane, 2017; Hidayathulla Khan et al. 2018; El Moutaouakil et al. 2020; Cianfrini et al. 2015; Hasnaoui et al. 1992; Lee & Ha, 2006; Zheng et al. 2021; etc.) have also considered some of these flows with different configuration and can be studied for more insight.

However, Ongodiebi & George, (2025) and George & Dienagha, (2025) in recent times have focused on the mixing pattern of free convection flow in warm bathing water where density was assumed to be a quadratic function of temperature. The pattern in their result appeared very similar to those by Cianfrini et al. 2015 with a similar configuration which also conform with real life scenario. But then, apart from the analysis on the flow pattern, and as well the temperature, vertical and horizontal velocity profiles, their simulations could not capture the point where hot water at the upper section of the container deplete completely. Furthermore, determining the various profiles at different levels is also important so as to give a detailed analysis on the temperature gradient. Finally, are the results dependent or independent of any flow parameter? Thus, we will consider these limitations as highlighted above by proposing a numerical simulation with the same configuration and all the assumptions as recorded in the literature by Ongodiebi & George, (2025) and George & Dienagha, (2025) are the same. The flow parameters are also the same except for the Reynold's number Re that will be varied for $5 \leq Re \leq 110$ for a laminar flow scenario. This investigation will enable us to gain more insight into the mixing pattern of both the hot and cold water as they come in contact in our daily warm bathing water. The key behaviour to expect is a natural convection flow even as any part of the fluid close to Tm descend from the top as both fluid mixes further. We can further study the literature by Ongodiebi & George, (2025) for more understanding.

Model Formulation and Governing Equations

The mixing pattern of free convection flow is into consideration as cold and hot water come in contact. As time progresses, it will be very obvious that any fluid mixture that have mixed up to Tm will form a descending plume due to the nonlinear relation between density ρ and temperature T in water. Thus, in order for us to depict the real flow free convection scenario, we are proposing a quadratic dependence relation assumption of density on temperature as also proposed in the work by Ongodiebi & George, (2025) and George & Dienagha, (2025) l

$$\rho = \rho m - \beta(T - Tm)2. \quad (1)$$

The quadratic dependence relation assumption have shown to gives a good fit to experimentally determined density in fresh water at temperatures below $10^{\circ}C$, *taken* $Tm = 3.98^{\circ}C$, $\rho m = 1.000 \times 10^3\ kg.m^{-3}$ *and* $\beta = 8.0 \times 10^{-3}\ kg.m^{-3}(^{\circ}C)^{-2}$

(Ongodiebi & George, 2025 and George & Dienagha, 2025; Moore & Weiss, 1973; Oosthuizen & Paul, 1996) and all other fluid properties such as viscosity, thermal diffusivity are assumed constant. We assume that the flow is two dimensional and time dependent with liquid property being constant except for the water density, which changes with temperature. We can non-dimensionalise the coordinates x, y, velocity components u, v, time t, pressure p and temperature T by.

$$U = \frac{u}{U_*} \quad V = \frac{v}{U_*} \quad X = \frac{x}{H} \quad Y = \frac{y}{H} \quad \tau = \frac{t}{\frac{H}{U_*}} \quad P = \frac{p}{\rho U_*^2}$$

$$\phi = \frac{T - T_\infty}{T_m - T_\infty}, \quad (2)$$

Where x and u are horizontal, y and v are vertical; $U_* = \sqrt{\frac{\rho_\infty - \rho}{\rho} H}$ is the relative frontal velocity and domain height H. We also define dimensionless parameters, the Reynolds Re, Prandtl Pr and Froude Fr numbers, by

$$\nu = \frac{\mu}{\rho} \quad \alpha = \frac{k}{\rho c_p} \quad Re = \frac{U_* H}{\nu} \quad Pr = \frac{\nu}{\alpha} \quad Fr^2 = \frac{\rho_m U_*^2}{g\beta(T_m - T_\infty)^2 H}, \quad (3)$$

where ν and α are the respective diffusivities of momentum and heat, and μ is viscosity, k is thermal conductivity and cp is specific heat capacity. With the dimensionless variables and parameters, the continuity equation, horizontal and vertical momentum equations and thermal energy equation are given as

$$\frac{\partial U}{\partial X} + \frac{\partial V}{\partial Y} = 0 \quad (4)$$

$$\frac{\partial U}{\partial \tau} + U\frac{\partial U}{\partial X} + V\frac{\partial U}{\partial Y} = -\frac{\partial P}{\partial X} + \frac{1}{Re}\left(\frac{\partial^2 U}{\partial X^2} + \frac{\partial^2 U}{\partial Y^2}\right) \quad (5)$$

$$\frac{\partial V}{\partial \tau} + U\frac{\partial V}{\partial X} + V\frac{\partial V}{\partial Y} = -\frac{\partial P}{\partial Y} + \frac{1}{Re}\left(\frac{\partial^2 V}{\partial X^2} + \frac{\partial^2 V}{\partial Y^2}\right) + \frac{1}{Fr^2}[\phi^2 - 2\phi] \quad (6)$$

$$\frac{\partial \phi}{\partial \tau} + U\frac{\partial \phi}{\partial X} + V\frac{\partial \phi}{\partial Y} = \frac{1}{RePr}\left(\frac{\partial^2 \phi}{\partial X^2} + \frac{\partial^2 \phi}{\partial Y^2}\right) \quad (7)$$

Our computational domain is also consists of a domain length L of total L = 70, i.e., $0 \leq X \leq 70$, and a domain height H = 90 i.e., $0 \leq Y \leq 90$. Where the domain length and height of the hot upper section is L1 = 70 and H1 = 7 respectively: while, the ambient fluid domain length and height is L = 70 and H = 80. All side walls and the horizontal base of the container are considered insulated with a surface condition that is considered adiabatic.

Therefore, our initial conditions are an undisturbed, homogeneous medium,

$$U = 0, \quad V = 0, \quad \phi = 0, \quad \text{for the cold section} \quad \tau < 0 \quad (8)$$

And

$$U = 0, \quad V = 0, \quad \phi = 2.5, \quad \text{for the hot section} \quad \tau < 0 \quad (9)$$

For $\tau \geq 0$ we have boundary conditions as follows. On the side walls:

$$U = 0, \quad V = 0, \quad \frac{d\varphi}{dX} = 0 \quad (10)$$

At the interaction layer (source):

$$U = 0, \quad V(X, 0) = 1, \quad \varphi = 2.5 \text{ for } L_1 \text{ and } \varphi = 0 \text{ for } L, \quad \text{for } X = 70, \text{ at } Y = H_1 \text{ and } H \text{ respectively.} \quad (11)$$

On the floor of the domain:

$$U = 0, \quad V = 0, \quad \frac{\partial \varphi}{\partial Y} = 0 \quad (12)$$

At the top of the domain:

$$\frac{\partial U}{\partial Y} = 0, \quad V = 0, \quad \frac{\partial \varphi}{\partial Y} = 0 \quad (13)$$

Varying Reynolds number within $5 \leq Re \leq 110$, Froude number Fr = 2.5 and Prandtl number Pr = 9.5 all will be kept fixed throughout the investigation. The dimensionless temperature φ = 2.5 in the L1 is equivalent to a temperature at 10°C placed at the surface of an ambient temperature 0°C. Result is by means of COMSOL Multiphysics software. It is a commercial software that uses the

finite element solver with discretization by the Galerkin method and stabilisation to prevent spurious oscillations. Our results here are independent of the mesh used, if only the mesh size is ≤ 0.05. More information about the numerical methods is available from the COMSOL Multiphysics website (COMSOL Multiphysics Cyclopedia, 2016). Results will be presentation will by surface temperature plots of dimensionless temperature on a colour scale from dark red for the ambient temperature φ = 0.0, through yellow to white for the source temperature φ = 2.5. Note that φ = 1.0 corresponds to the temperature of maximum density while φ = 2.0 is the temperature at which warm water has the same density as the ambient cold water.

Numerical Results

The evolution of temperature field for a free convection flow is studied in a warm bathing water numerically and shown in Figure 1, 2 & 3 for a range of Reynolds number 0 ≤ Re ≤ 110, keeping Fr = 2.5 and Pr = 9.5 fixed throughout the study for a laminar flow scenario. The results as shown in Fig. 1, 2 & 3 are for Re = 5, 50 & 110 respectively. After the start of the simulation, cabbeling process begins at the contact layer where both hot and cold water come in contact. But this is more evident as time progresses (see Fig., 1(c), 2(b) & 3(b)). But then, the results in Fig. 2(b) & 3(b) showed that slightly significant mixed fluid is produced already as compared to that in Fig. 1(c). This implies that slightly vigorous had occur owing to the increasing Re, even though, the velocity in such free convection flows are usually small. As the simulation progresses further, much dense fluid that have attained Tm or a temperature closed to it is produced at the mixing layer that sinks in the form of an inverted mushroom like structure to the bed of the domain (see Fig., 1(d & e), 2(c & d) and 3(c & d)). Note, we have come to understand that water around a heat source gain heat and form buoyancy flow, if the heat source is within the ambient fluid. In the case where the ambient water is below Tm as it is in the present configuration the ambient cold water will move to replace the initial fluid at the contact zone as dense fluid continue to sink to the bed. This process continue until the entire domain water gets warm as also contained in the literature by Kane, (2017), Nayak et al. (2018), Ongodiebi & George, (2025), George & Dienagha, (2025), Cianfrini et al. (2015). This is because, the sinking warm but dense water interact further with the domain fluid inducing it. As time further progresses, it was observed that the volume of hot water at the upper section had completely depleted while the entire ambient water temperature had also increased through convection and the entire domain water is shown to have attained a relatively the same temperature without any external influence or mixing force. (see Fig., 1(g), 2(f) and 3(g)). This (the upper section had completely depleted) was not captured in the results by Ongodiebi & George, (2025), George & Dienagha, (2025). It is also interesting to note that the time rate of hot water depletion vary with Reynolds number. That is, as Reynolds number increases, rate at which the hot water depletes increases at initial time with Re but later decreases with Re; and it is evident in Fig. 1(g), 2(f) and 3(f) at dimensionless time τ = 350. This might be as a result of the quick production of dense fluid with increasing Re. That is, as much dense fluid was produced at earlier time interval, this further induces the ambient water changing its initial temperature affecting the later mixing rate. Remember that just a little mixing is

required for temperature between 0°C and 10°C to attain Tm. Thus, as the domain temperature increased, it in turn decreases the mixing rate at much later time. Whereas, slightly slow mixing for the lower Re which in turn leads to slow production of dense fluid. Therefore, the time it take for dense fluid to sink to the bed for smaller Re is slightly longer

as compared to the time it takes as Re increases which is also evident in figure 7. To this end, we can conveniently state that our results here are dependent on Reynolds number as there might be the likelihood of different regimes of mixing. Free convection flows with this configuration had received less attention except for Cianfrini et al. (2015), Ongodiebi & George, (2025) and George & Dienagha, (2025) with similar configuration. The results by Ongodiebi & George, (2025) and George & Dienagha, (2025) where density was taken as a quadratic function of temperature appears very close as compared to our present results. The main difference in our present result is the decrease in mixing in later time interval as Re increases; which in turn leads to a delay in the time taken for total depletion of the hot water at the upper most part . Meanwhile, for Re ≥ 50, it is expected that significant dense fluid could be produced at earlier time as also observed in the results by George & Dienagha, (2025) owing to the slight increase in the mixing rate.

Temperature profiles were also considered at some levels (X, 69; 30; 10) below the contact layer and plotted against the x-coordinate for a detailed analysis as shown in figure 4, 8 & 9. Results in Fig. 4 at (X, 69) showed a strong agreement with the various observations from the temperature field (see Fig. 1(a & b), 2(a & b) and 3(a & b): that there was no or insignificant sinking dense fluid at dimensionless time τ = 10 & 50 for all the Re cases shown. But as time progresses, more significant descending dense and mixed fluid with different temperature were found within the indicated time inter- val. Meaning that even though cabbeling begins immediately after the start of the simulation at the earliest time interval, significant dense fluid have not been produced that descends. In a similar manner, the results in Fig. 8 & 9 at (X, 30 & 10) also agrees with the various observations from the temperature field (see Fig. 1, 2 and 3). that no descending dense fluid at dimensionless time τ = 10, 50, 100 & 150 was found for various Re. Temperature in the mixed fluid at these levels also showed that the fluid temperature is approximately the same everywhere. Confirming the fact that the entire domain fluid.

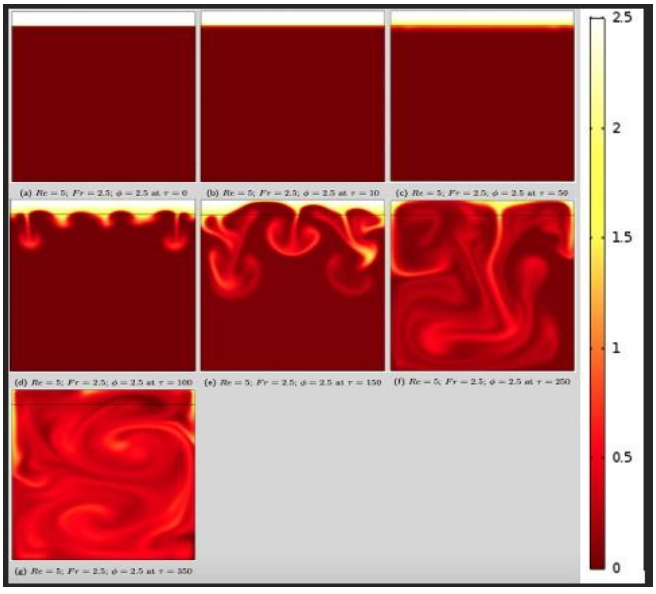

Fig. 1: Evolution of temperature field in Laminar convective flow in warm bathing water for Re = 5, Fr = 2.5 and Prandtl number Pr = 9.5 and dimensionless temperature φ = 2.5 at the upper section within the time range 0 ≤ τ ≤ 350.

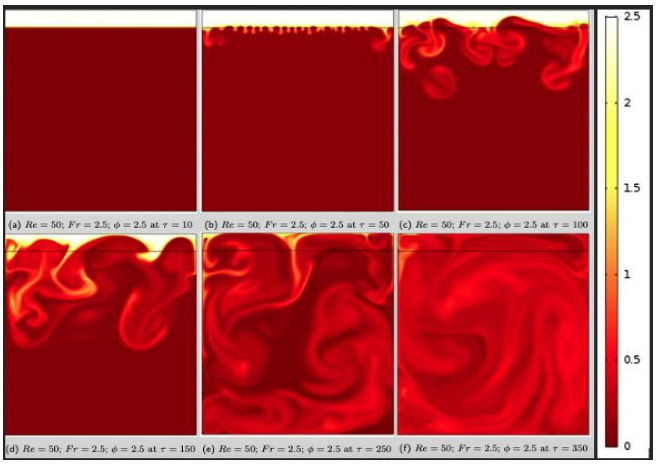

Fig. 2: Evolution of temperature field in Laminar convective flow in warm bathing water for Re = 50, Fr = 2.5 and Prandtl number Pr = 9.5 and dimensionless temperature φ = 2.5 at the upper section within the time range 10 ≤ τ ≤ 350

will become the same with time. This means that the more the interaction between the two fluid, the more the hot water get depleted through mixing inducing the entire surrounding fluid. Fluctuations in the temperature profiles also describes the fluid movement as both hot and cold fluid mixes further in all direction: and this in turn leads us to discussing the velocity profiles in both the x-component and y-component.

Profiles of x-component and y-component velocities were also determined at (X, 69) for the various Re cases as considered and plotted against the x-coordinate as shown in figure 5 & 6. The x-component velocity showed that there was a fluid movement in all directions horizontally, owing to the fact that the warm but dense descending fluid in vortex form continue to interact with the ambient fluid even as it descends. But then, there was no fluid motion in the earlier time interval (see Fig. 6 (a) & (b)) as compared to that in figure 6(c). Furthermore, the fluctuations in the curves differs as Re varies, which is reasonable as descending warm but dense plume continue to draw surrounding fluid into itself depleting further downwards; as also recorded in the literature by Ongodiebi & George, (2025) and George & Dienagha, (2025). In a similar manner, the y-component velocities also showed that there was no descending mixed fluid at dimensionless time τ = 10 for all the Re cases. but then, as time increases the mixing rate also increases slightly with Re as it is evident in figure 1 - 3 which corresponds to those in figure 5(a - c). Fluctuations in the curves indicates that even as the dense fluid continue to descend, fluid that is still positively buoyant moves upwards. This behaviour in the y-component velocity profile was also observed in the results by George & Dienagha, (2025) and Ongodiebi & George, (2025). Maximum time taken for descending dense fluid to reach domain floor and the time taken to attain that depth are tabulated for a range of Reynolds numbers up to 110 in Figure 10 Table 1, and plotted in Figs. 7 Our empirically determined data set could allow us to identify a single regime of Re-dependence with any confidence. This is shown by the straight line in Figs. 7, which represent best fit power law obtained by linear regression of logRe on logτn.

$$Re = 223.72\tau^{(-0.021)}\ [R^2 = 0.1021] \qquad (14)$$

where R^2 is the regression coefficient. This result also confirm the fact that production of dense fluid slightly increases with Reynolds number and as such the time taken for dense fluid to reach the floor is a bit shorter as compared to smaller Reynolds number. Thus, all the behaviours as described in this present investigation are dependent on the Reynolds number. But then, we are suggesting that other flow parameter such as the Froude number should be varied to know if a different regime of flow exist. The results as presented here are very good with in-depth analysis as they properly describe the real flow scenario for better insight into the mixing behaviour in a free convection flow through our daily warm bath.

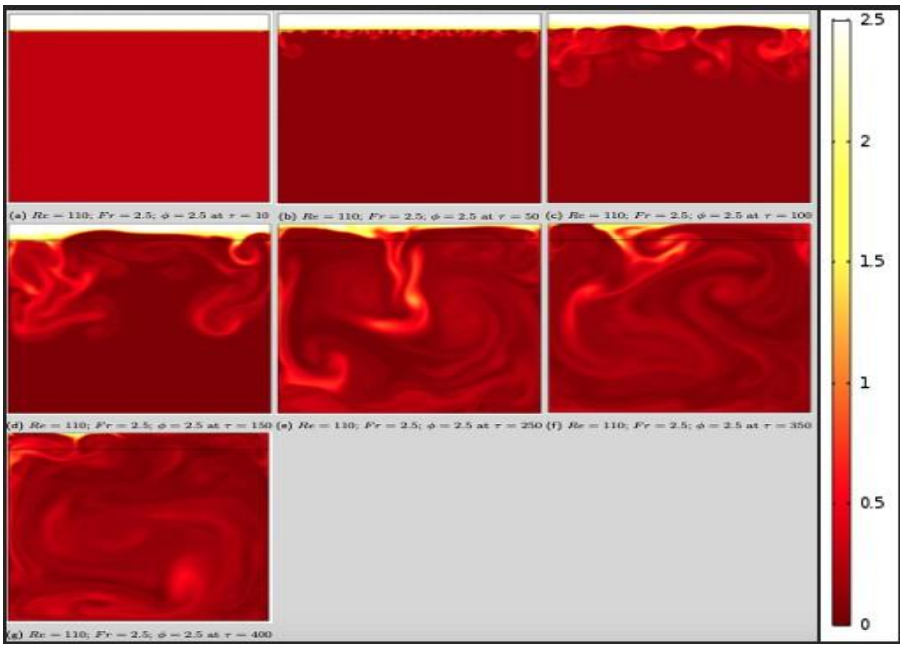

Fig. 3: Evolution of temperature field in Laminar convective flow in warm bathing water for Re = 110, Fr = 2.5 and Prandtl number Pr = 9.5 and dimensionless temperature φ = 2.5 at the upper section within the time range 10 ≤ τ ≤ 400

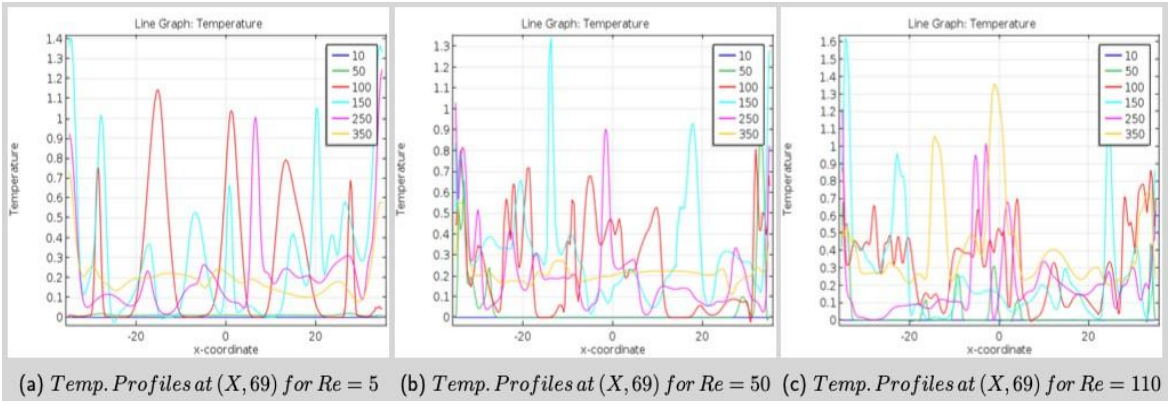

(a) $Temp. Profiles\ at\ (X, 69)\ for\ Re = 5$ (b) $Temp. Profiles\ at\ (X, 69)\ for\ Re = 50$ (c) $Temp. Profiles\ at\ (X, 69)\ for\ Re = 110$

Fig. 4: Dimensionless Temperature profiles at some point close to the mixing layer T (X, 69) at time τ = 20, 50, 100, 200, 250

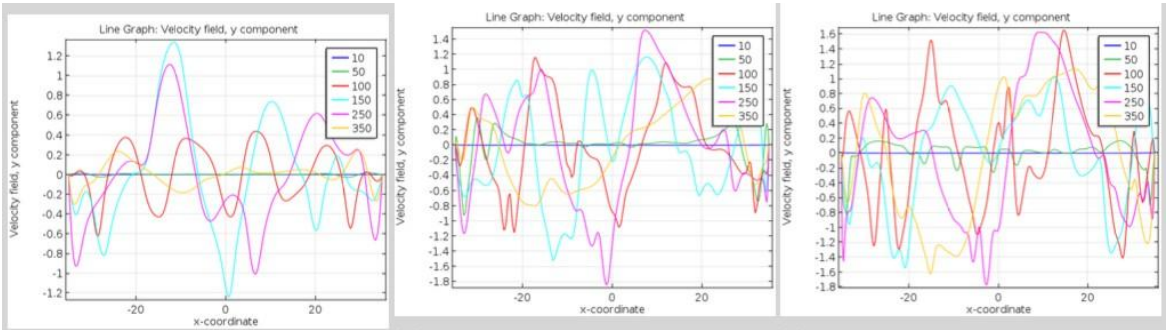

(a) $Y - Velo. Profiles\ at\ (X, 69)\ for\ Re = 5$ (b) $Y - Velo. Profiles\ at\ (X, 69)\ for\ Re = 50$ (c) $Y - Velo. Profiles\ at\ (X, 69)\ for\ Re = 110$

Fig. 5: Dimensionless vertical velocity profiles at some point close to the mixing layer V (X, 69) at time τ = 20, 50, 100, 200, 250

In conclusion, whenever water masses of different densities meet, mixing will take place without any perturbation until the entire surrounding fluid is induced through convection flow as we have shown.

Discussion/Conclusion

A detailed study of Laminar free convection flow in warm bathing water had just been carried out taken density as a quadratic function of temperature. This study was for a range of Reynolds number $0 \leq Re \leq 110$ for a practical laminar flow case, keeping Fr = 2.5 and Pr = 9.5 fixed throughout the study. The results here showed that cabbeling begins immediately hot and cold water come in contact at the contact layer. The cabbeling behaviour changes slightly with Re owing to the increasing Re, even though, the velocity in such free convection flows are usually small. Dense fluid that have attained Tm or a temperature closed it descending to the floor of the domain. It was also observed that the volume of hot water at the upper section at some point depleted completely and in turn the entire ambient water temperature increased through convection and as well maintain a relatively the same temperature everywhere without any external influence. The results here requires just a little mixing for temperature between 0°C and 10°C to attain Tm. As the domain temperature increased, it in turn decreases the mixing rate at much later time. Whereas, slightly slow mixing for the lower Re which in turn leads to slow production of dense fluid at the contact layerj. Thus, the time it take for dense fluid to sink to the bed for smaller Re is slightly longer as compared to the time it takes as Re increases. Temperature profiles were also analysed at some points (X, 69; 30; 10) below the contact layer and plotted against the x-coordinate for a detailed analysis as shown in figure 4, 8 & 9. and as well the profiles of x-component and y-component velocities were also determined at (X, 69) for the various Re cases as considered and plotted against the x-coordinate as shown in figure 5 & 6. These profiles also agrees with the behaviours as described from the Temperature field. Where fluctuations.

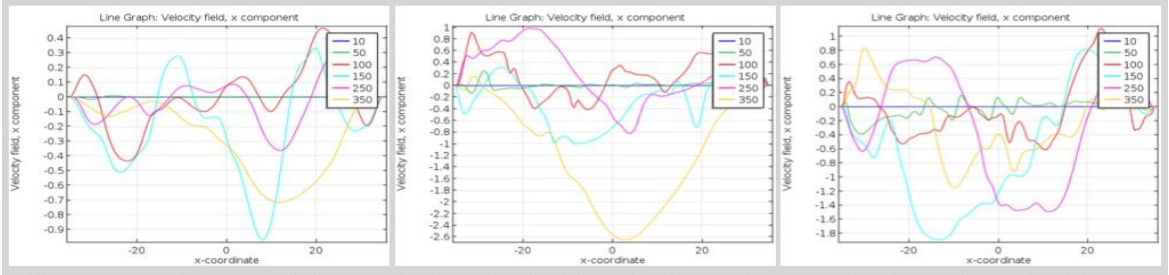

(a) $X - Velo. Profiles\ at\ (X, 69)\ for\ Re = 5$ (b) $X - Velo. Profiles\ at\ (X, 69)\ for\ Re = 50$ (c) $X - Velo. Profiles\ at\ (X, 69)\ for\ Re = 110$

Fig. 6: Dimensionless horizontal velocity profiles at some point close to the mixing layer V (X, 69) at time τ = 20, 50, 100, 200, 250

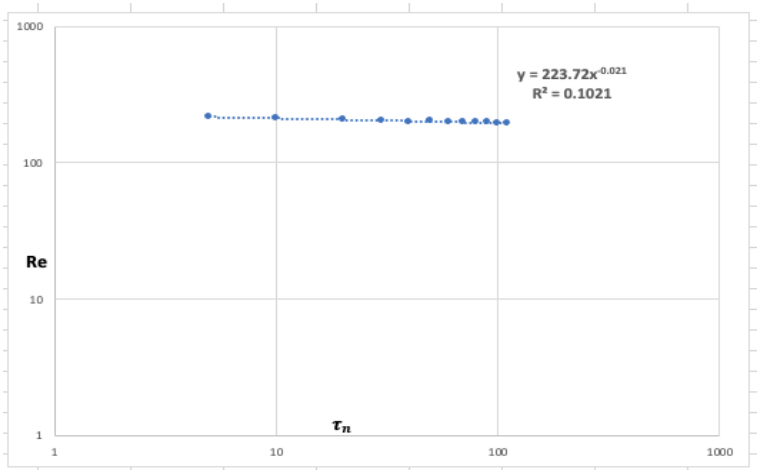

Fig. 7: Reynold number Re vs Maximum time taken for descending plume to reach domain floor

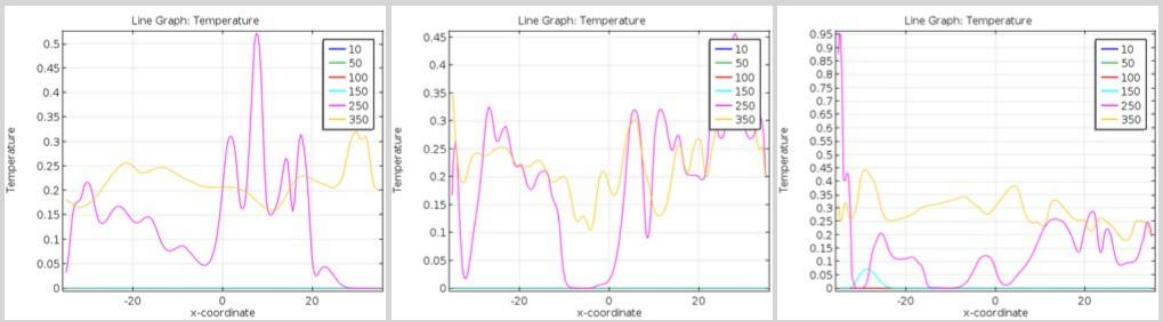

(a) $Temp.Profiles\,at\,(X,30)\;for\;Re=5$ (b) $Temp.Profiles\,at\,(X,30)\;for\;Re=50$ (c) $Temp.Profiles\,at\,(X,30)\;for\;Re=110$

Fig. 8: Dimensionless Temperature profiles at some point T (X, 30) away from the contact layer at time τ = 20, 50, 100, 200, 250

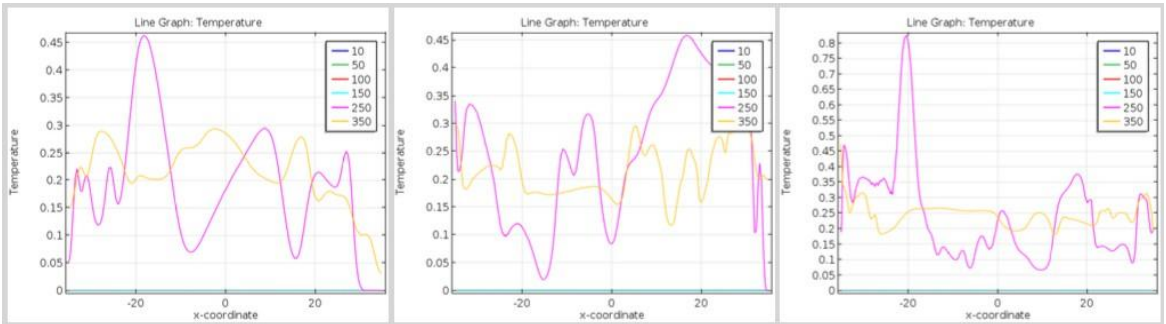

(a) $Temp.Profiles\,at\,(X,10)\;for\;Re=5$ (b) $Temp.Profiles\,at\,(X,10)\;for\;Re=50$ (c) $Temp.Profiles\,at\,(X,10)\;for\;Re=110$

Fig. 9: Dimensionless Temperature profiles at some point T (X, 10) away from the contact layer at time τ = 20, 50, 100, 200, 250

Table 1. Maximum time taken for descending plume to reach domain floor for the various Reynolds Numbers

Reynolds No. (Re)	Dimensionless Time (τ)
5	217.5
10	212.5
20	205
30	201
40	200
50	203
60	199
70	200
80	198
90	198
100	195
110	193

Fig. 10: Table 1. Maximum time taken for descending plume to reach domain floor for the various Reynolds Numbers

in the temperature profiles describes the fluid movement as both hot and cold fluid mixes further in all direction: while, fluctuations in the curves for the y-component velocity profile indicates that even as the dense fluid continue to descend, fluid that is still positively buoyant moves upwards. The maximum time taken for descending dense fluid to reach domain floor and the time taken to

attain that depth were also considered. Our empirically determined data set allow us to identify a single regime of Re-dependence and shown by the straight line in Figs. 7, which represent best fit power law obtained by linear regression of logRe on logτn (see equation). In conclusion, these results are very good as they presents us with the real flow scenario for better insight into the cabbeling phenomenon in a free convection flow through our daily warm bath.

References

1. Brownridge, J. D. and Robinson, D. B. J. (2019). Experimental Investigation of Upside down Convection and Metastable Convection Cell in Water. International Journal of Advanced Research in Science, Engineering and Technology, **6** (1), Pp. 7777 – 7788.
2. Charqui, Z., Boukendil, M., El Moutaouakil, L. and Zrikem, Z. (2021). Numerical Investigation of the Flow and Heat Transfer Generated by Natural Convection and Surface Radiation in an Open Enclosure . In Proceedings of the 2nd International Conference on Big Data, Modelling and Machine Learning, Pp. 371 -375.
3. Cianfrini, C., Corcione, M., Habib, E. and Quintino, A. (2015) Natural Convection of Water near 4°C in a Bottom-Cooled Enclosure . Energy Procedia **82** Pp. 322 – 327.
4. COMSOL Multiphysics Cyclopedia. The Finite Element Method (FEM). [ONLINE] Available at: https://www.comsol.com/multiphysics/finite-element-method [Accessed 28 April 2016].
5. Djoubeir, D., Omar, K., Soufien, C. and Saadoun, B. (2014) Numerical Simulation of Nat- uralConvection in a Square Cavity with Partially Active Vertical and Horizontal Walls. https://www.semanticscholar.org/paper/Numerical-Simulation-of-Natural-Convection-in-a-and-Djoubeir-Omar/b05c2ddd1dcd1f89d48084f3126527732d5f3e72 **2.** Pp. 1 – 6.
6. El Moutaouakil, L., Boukendil, M., Zrikem, Z. and Abdelbaki, A. (2020) Natural Convection and Sur- face Radiation Heat Transfer in a Cavity with Vertically Oriented Fins . Materialstoday: Proceedings https://doi.org/10.1016/j.matpr.2020.03.526 **27**(4) Pp. 3051 – 3057.
7. Ezan, A. M. and Kalfa, M. (2017). Natural Convection Of Water Near 4°C Inside Partially Heated And Cooled Vertical Walls . Journal of Theermal Science and Technology, **37** (1), Pp. 1 -12.
8. George, M. A. and Osaisai, F. E. (2022). Density Current Simulations In Cold Fresh Water And Its Cabbeling phenomenon: A Comparative Analysis With Given Experimental Results Current Journal of Applied Science and Technology **41**(29) Pp. 37 – 52.
9. George, M. A. and Dienagha, N. (2025). The mixing Behaviour of Laminar Convection flow in Warm Bathing Water: An In-depth Review GRS Journal of Multidisciplinary Research and Studies, **2**(12) Pp. 11 – 17.
10. Gopalakrishnan, N., Prasad, B. V. S. S. S. and Srinivasa Murthy, S. (2005). Natural Convection in Stratified Hot Water Storage Tanks Current Journal of Applied Science and Technology **41**(29) Pp. 37 – 52.
11. Hasnaoui, M., Bilgen, E. and Vasseur, P. (1992) Natural Convection Heat Transfer Rectangular Cavities Partially Heated from Below . Journal of Thermophysics and Heat Transfer **6**(2) Pp. 255 – 264.
12. Hidayathulla Khan, B. M., Venkatadri, K., Anwar Bég, O., Ramachandra Prasad, V., & Mallikarjuna, B. (2018). Natural convection in a square cavity with uniformly heated and/or insulated walls using marker-and-cell method. *International Journal of Applied and Computational Mathematics*, *4*(2), 61.
13. Hossain, M. A., & Rees, D. S. (2005). Natural convection flow of water near its density maximum in a rectangular enclosure having isothermal walls with heat generation. *Heat and mass transfer*, *41*(4), 367-374.
14. Kane, M. , Mbow, C. , Sow, M. and Sarr, J. (2017) A Study on Natural Convection of Air in a Square Cavity with Partially Thermally Active Side Walls . Journal of Fluid Dynamics **7** Pp. 623 – 641
15. Khanorkar, M. P. and Thombre, E. R. (2013) CFD Analysis of Natura Convection Flow Through Vertical Pipe . International Journal of Mechanical Engineering and Robotics Research 2(3) Pp. 371 – 378.
16. Khurshid, H. and Silaipillayarputhur, K. (2018) A Study on the Solar Radiation Incident upon the Overhead water tanks in Saudi Arabia with Different Configurations . International Journal of Engineering & Technology **7**(3) Pp. 991 – 995.
17. Lee, R. J. and Ha, Y. M. (2006) Numerical simulation of natural convection in a horizontal enclosure with a heat-generating conducting body . International Journal of Heat and Mass Transfer **49** Pp. 2684 – 2702.
18. Li, Y., Yuan, X., Wu, C. and Hu, Y. (2011). Natural convection of water near its density maximum between horizontal cylinders . International Journal of Heat and Mass Transfer, **54.**
19. Moore, D. R. and Weiss, N. O. (1973). Nonlinear penetrative convection. Journal of Fluid Mechanics, 61 Pp. 553- 581.
20. Nayak, C. R., Roulb, K. M. and Sarang, K. S. (2018) Natural convection heat transfer in heated vertical tubes with internal rings. Journal of Polish Academy of Science **39**(4) Pp. 85 -111.
21. Ongodiebi, Z. and George, M. A. (2025) Numerical Simulation of Convection flow in Warm Bath and Its Possible mixing Behaviour. International Journal of Mathematics and Computer Research **13**(03) Pp. 4968 – 4974.
22. Oosthuizen, P. H. and Paul, J. T. (1996). A Numerical study of the Steady State Freezing of Water in an open Rectangular Cavity. International Journal of Numerical Methods for Heat and Fluid Flow, **6** (5), Pp. 3-16.
23. Radhwan, M. A and Zaki, M. G. (2000) Laminar Natural Convection in a Square Enclosure with Discrete Heating of Vertical Walls. Journal of King Abdulaziz University-Engineering Sciences **12**(2) Pp. 83 – 99.
24. Rahman, M. M., Mamourian, M., Mirzakhanlari, S., Rahimi, A. B. and Ellahi, R. (2017) Numerical Study of Surface Radiation and combined Natural Convection heat transfer in A Solar Cavity receiver . Journal of Naval Architecture and Marine Engineering **7** Pp. 37 – 50.
25. Shirvan, K. M., Mamun, H. A. M., Billah, M. M. and Saidur, R. (2010) Natural Convection Flow In A Square Cavity With Internal Heat Generation And A Flush Mounted Heater On A Side Wall . International Journal of Numerical Methods for Heat and Fluid Flow.

26. Singh, O., Singh, S. and Kedare, S. B. (2016) Effect on Thermal Radiation on Accuracy of restricted Domain Approach in a Square Open Cavity. In Proceedings of the ASME 2016 International Mechanical Engineering Congress and Exposition.

27. Zheng, J., Zhang, L., Yu, H., Wang, Y. and Zhao, T. (2021) Study on Natural Convection Heat Transfer in a Closed Cavity with Hot and Cold Tubes. Science Progress **104**(2) Pp. 1 – 25.